

## X-Ray Structural Characterization of the Bis-Guanine Derivative of a Cisplatin Analogue Having Just One Proton on Each Coordinated Nitrogen and a Head-to-Head Conformation: [Pt{(±)-*N,N'*-Dimethyl-2,3-diaminobutane}(9-ethyl-guanine)<sub>2</sub>]dinitrate

Francesco P. Intini,<sup>†</sup> Renzo Cini,<sup>‡</sup> Gabriella Tamasi,<sup>‡</sup> Michael B. Hursthouse,<sup>§</sup> Luigi G. Marzilli,<sup>||,⊥</sup> and Giovanni Natile<sup>\*†</sup>

<sup>†</sup>Dipartimento Farmaco-Chimico, Università di Bari, Via E. Orabona 4, 70125 Bari, Italy,

<sup>‡</sup>Dipartimento di Chimica, Università di Siena, Via A. Moro 2, I-53100 Siena, Italy,

<sup>§</sup>School of Chemistry, University of Southampton, Southampton, SO17 1BJ, United Kingdom,

<sup>||</sup>Departments of Chemistry, Louisiana State University, Baton Rouge, Louisiana 70803, and

<sup>⊥</sup>Emory University, Atlanta, Georgia 30322

Received May 15, 2010

The X-ray structural and NMR characterization of a bis-guanine derivative of a cisplatin analogue designed to reduce the rate of the Pt–N7 rotation of the coordinated guanine nucleobases by more than 1-million-fold is reported. The [Pt{(±)-Me<sub>2</sub>dab}(9-EtG)<sub>2</sub>](NO<sub>3</sub>)<sub>2</sub> (Me<sub>2</sub>dab = *N,N'*-dimethyl-2,3-diaminobutane, 9-EtG = 9-ethyl-guanine) complex crystallizes in the *P2<sub>1</sub>/n* space group, and the crystal contains a racemic mixture of complex molecules. The data were collected at 120 ± 2 K, and the crystal and molecular structure (comprising one disordered nitrate) were resolved and refined to conventional agreement factors of R1 = 0.0270 and wR2 = 0.0565. The guanine ligands assume the less common head-to-head (HH) orientation, disclosing full details of the intramolecular relationships between *cis* guanines and between guanine and *cis* amine. Moreover, an understanding has been gained of the steric factors determining induction of asymmetry (from carbons to adjacent nitrogen atoms) and puckering of the chelate ring ( $\delta$  or  $\lambda$  for *R,S,S,R* or *S,R,R,S* configurations at the N,C,C,N chelate-ring atoms, respectively) within the Me<sub>2</sub>dab ligand. The chemical shift separation between H8 signals of the two HT atropisomers and between the two H8 signals of the single HH atropisomer can be explained in terms of canting of the nucleobases relative to the coordination plane and in terms of the different relationships between the H8 proton of one guanine and the shielding zone of the *cis* guanine. Furthermore, for each configuration of the Me<sub>2</sub>dab ligand (*R,S,S,R* or *S,R,R,S*), the NMR data indicate that the handedness of canting is similar for the two guanines in all three (two HT and one HH) conformers (*R* canting for *R,S,S,R* and *L* canting for *S,R,R,S* configuration).

### Introduction

The serendipitous discovery by Rosenberg et al. of the antitumor activity of *cisplatin* (*cis*-diamminedichloridoplatinum(II))<sup>1–3</sup> was a breakthrough in the chemotherapy of tumors. This highly effective drug for the treatment of testicular and ovarian cancers is beneficial, in association with other antitumor drugs, also in the treatment of many other types of tumors.<sup>4</sup>

Thousands of platinum compounds have been synthesized and tested for antitumor activity in an attempt to circumvent the acquired or intrinsic resistance to *cisplatin* of several

tumors. Dozens of new platinum drugs have entered human clinical trials,<sup>5</sup> but only *carboplatin* [*cis*-diammine(1,1-cyclobutanedicarboxylato-*O,O'*)platinum(II)], which is active in the same range of tumors as *cisplatin* but with lower toxicity,<sup>5</sup> and *oxaliplatin* [(*R,R*)-1,2-diaminocyclohexane(oxalato-*O,O'*)platinum(II)],<sup>5,6</sup> approved for the secondary treatment of metastatic colorectal cancer,<sup>5,6</sup> have achieved worldwide routine clinical use.

DNA remains the ultimate target for *cisplatin*, which forms adducts mainly with N7 of adjacent purines.<sup>6–10</sup> This lesion

\*To whom correspondence should be addressed. Phone: 0039-080-544-2774. Fax: 0039-080-544-2230. E-mail: natile@farmchim.uniba.it.

(1) Rosenberg, B.; Van Camp, L.; Krigas, T. *Nature* **1965**, *205*, 698–699.  
(2) Rosenberg, B.; Van Camp, L.; Grimley, E. B.; Thomson, A. J. *J. Biol. Chem.* **1967**, *242*, 1347–1352.

(3) Rosenberg, B. *Plat. Met. Rev.* **1971**, *15*, 42–51.

(4) Weiss, R. B.; Christian, M. C. *Drugs* **1993**, *46*, 360–377.

(5) Lebwohl, D.; Canetta, R. *Eur. J. Cancer* **1998**, *34*, 1522–1534.

(6) Hambley, T. W. *Coord. Chem. Rev.* **1997**, *166*, 181–223.

(7) Reedijk, J. *Chem. Commun.* **1996**, 801–806.

(8) Jamieson, E. R.; Lippard, S. J. *Chem. Rev.* **1999**, *99*, 2467–2498.

(9) Ano, S. O.; Kuklennyk, Z.; Marzilli, L. G. In *Cisplatin: Chemistry and Biochemistry of a Leading Anticancer Drug*; Lippert, B., Ed.; Wiley-VCH: Weinheim, Germany, 1999; pp 247–291.

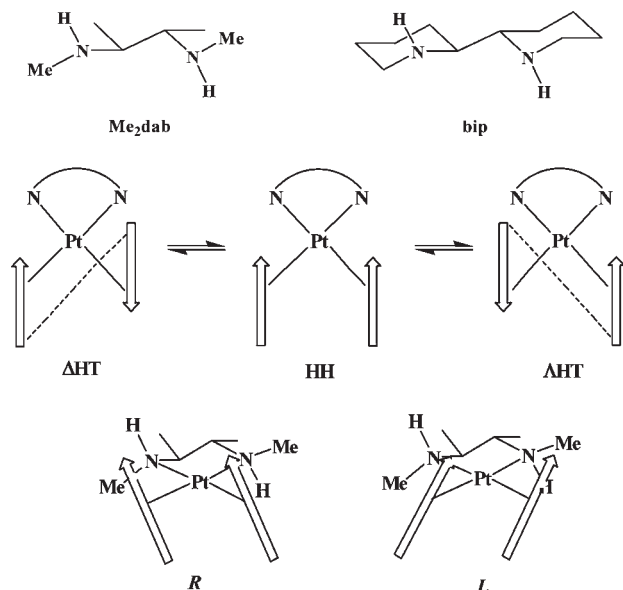


**Figure 1.** Schematic drawing of  $\text{Me}_2\text{dab}$  and **bip** ligands (top), of possible conformers (head-to-head, **HH**, and head-to-tail, **HT**) for complexes with two *cis* untethered guanine ligands (middle, arrows with the tip representing **H8**) and of *R* and *L* canting of the nucleobases (bottom, *R,S,R* configuration of  $\text{Me}_2\text{dab}$ ).

seems responsible for cell death, but the mechanism of action is not entirely understood.

In solution,  $\text{cis-A}_2\text{PtG}_2$  complexes ( $\text{A}_2$  = two amines or a diamine and  $\text{G}_2$  = two detached or tethered guanine bases) usually exhibit unrestricted rotation about the  $\text{Pt-N7}$  bond.<sup>11–14</sup> This results in great complexity in the investigation of dynamic nucleos(t)ide complexes. The structure in the solid state may be very different from that in solution because of crystal-packing interactions. In solution, because of fast interconversion between possible conformers, only one set of signals, the average of those of individual conformers, is observed.

The “dynamic motion problem” led us to construct analogues of cisplatin with bulky ligands designed to reduce the dynamic motion by destabilizing the transition state for  $\text{Pt-N7}$  rotation. An important feature of the design was to minimize steric effects in the ground state equilibrium species to allow conformers likely to be present in dynamic  $\text{cis-A}_2\text{PtG}_2$  adducts to exist in the new adducts also. By reducing rotation rates by 1-million/billion-fold, these ligands enabled us to understand the adducts of the highly fluxional cisplatin drug with DNA constituents.<sup>15</sup>

*N,N'*-dimethyl-2,3-diaminobutane ( $\text{Me}_2\text{dab}$ ) was the first carrier ligand used in such a detailed NMR “retro model” study (Figure 1).<sup>16–18</sup> The 2,2'-bipiperidine ligand (**bip**), analogous to  $\text{Me}_2\text{dab}$  but more sterically hindering of the

rotation process, was able to decrease the dynamic motion roughly 1 billion times with respect to  $(\text{NH}_3)_2$  and *ca.* 100 times with respect to  $\text{Me}_2\text{dab}$  in  $\text{cis-A}_2\text{PtG}_2$  complexes.<sup>19–24</sup> The use of  $\text{Me}_2\text{dab}$  and **bip** ligands allowed the simultaneous observation, by  $^1\text{H}$  NMR spectroscopy, of all possible conformers (two **HT** and one **HH** conformer, except in the case of tethered guanines, where a second **HH** is also possible, Figure 1) that can be formed in  $\text{cis-A}_2\text{PtG}_2$  complexes with a  $\text{C}_2$ -symmetrical carrier ligand.

Notwithstanding the large contribution these ligands have given to the understanding of structure and dynamics of platinum adducts with nucleobases in nucleotides and DNA, until recently, no X-ray structure supporting the in-plane bulk of these ligands and the out-of-plane steric effects, which could influence the ground state equilibrium composition of different conformers present in dynamic  $\text{cis-A}_2\text{PtG}_2$  adducts, had been reported. Finally, we succeeded in crystallizing the  $[\text{Pt}(\text{dimethylmalonato})\{\pm\}\text{-}2,2'\text{-bipiperidine}]$  complex whose X-ray analysis has shown a **bip** ligand squeezed in the platinum coordination plane.<sup>25</sup> Attempts to crystallize adducts of **bip**-Pt with guanine bases, so as to highlight interligand interactions that are responsible for slowing down dynamic motion of coordinated nucleobases and influencing the stability of possible (**bip**) $\text{PtG}_2$  conformers, were unsuccessful.

We have now succeeded in crystallizing the  $[\text{Pt}\{\pm\}\text{-}\text{Me}_2\text{dab}\}\text{(9-EtG)}_2](\text{NO}_3)_2$  complex, containing the other chelate ligand that has contributed greatly to “retro model” studies. Furthermore, this complex not only contains two coordinated guanines, but these are in the rather rare head-to-head conformation, which has allowed us to unravel chiral amine-*cis* G interactions that fully account for NMR features. Although the crystal was affected by disorder at one nitrate anion, the selection of good quality crystals and adequate instrumentation, together with a careful choice of data collection conditions, has allowed us to reach remarkably low standard deviations on atomic positions and thermal parameters for most of the atoms.

## Experimental Section

**Apparatus.** NMR spectra were run on Bruker Instruments Avance DPX 300 and Avance II 600 MHz machines. Standard Bruker automation programs were used for two-dimensional NMR experiments.  $^1\text{H}$  chemical shifts were referenced to TMS by using the residual protic peak of the solvent as an internal reference (7.24 ppm for chloroform-*d* and 4.76 ppm for the

(10) Marzilli, L. G.; Saad, J. S.; Kuklenyik, Z.; Keating, K. A.; Xu, Y. *J. Am. Chem. Soc.* **2001**, *123*, 2764–2770.

(11) (a) Cramer, R. E.; Dahlstrom, P. L.; Seu, M. J. T.; Norton, T.; Kashiwagi, M. *Inorg. Chem.* **1980**, *19*, 148–154. (b) Cramer, R. E.; Dahlstrom, P. L. *J. Am. Chem. Soc.* **1979**, *101*, 3679–3681.

(12) (a) Marcelis, A. T. M.; Korte, H. J.; Krebs, B.; Reedijk, J. *Inorg. Chem.* **1982**, *21*, 4059–4063. (b) Marcelis, A. T. M.; van der Veer, J. L.; Zwetsloot, J. C. M.; Reedijk, J. *Inorg. Chim. Acta* **1983**, *78*, 195–203.

(13) Cramer, R. E.; Dahlstrom, P. L. *Inorg. Chem.* **1985**, *24*, 3420–3424.

(14) (a) Dijt, F. J.; Canters, G. W.; den Hartog, J. H. J.; Marcelis, A. T. M.; Reedijk, J. *J. Am. Chem. Soc.* **1984**, *106*, 3644–3647. (b) Miller, S. K.; Marzilli, L. G. *Inorg. Chem.* **1985**, *24*, 2421–2425.

(15) Natile, G.; Marzilli, L. G. *Coord. Chem. Rev.* **2006**, *250*, 1315–1331.

(16) Marzilli, L. G.; Intini, F. P.; Kiser, D.; Wong, H. C.; Ano, S. O.; Marzilli, P. A.; Natile, G. *Inorg. Chem.* **1998**, *37*, 6898–6905.

(17) Xu, Y.; Natile, G.; Intini, F. P.; Marzilli, L. G. *J. Am. Chem. Soc.* **1990**, *112*, 8177–8179.

(18) Kiser, D.; Intini, F. P.; Xu, Y. H.; Natile, G.; Marzilli, L. G. *Inorg. Chem.* **1994**, *33*, 4149–4158.

(19) Ano, S. O.; Intini, F. P.; Natile, G.; Marzilli, L. G. *Inorg. Chem.* **1999**, *38*, 2989–2999.

(20) Ano, S. O.; Intini, F. P.; Natile, G.; Marzilli, L. G. *J. Am. Chem. Soc.* **1997**, *119*, 8570–8571.

(21) Ano, S. O.; Intini, F. P.; Natile, G.; Marzilli, L. G. *J. Am. Chem. Soc.* **1998**, *120*, 12017–12022.

(22) Saad, J. S.; Scarcia, T.; Shinozuka, K.; Natile, G.; Marzilli, L. G. *Inorg. Chem.* **2002**, *41*, 546–557.

(23) Marzilli, L. G.; Ano, S. O.; Intini, F. P.; Natile, G. *J. Am. Chem. Soc.* **1999**, *121*, 9133–9142.

(24) Saad, J. S.; Scarcia, T.; Natile, G.; Marzilli, L. G. *Inorg. Chem.* **2002**, *41*, 4923–4935.

(25) Intini, F. P.; Cini, R.; Tamasi, G.; Hursthouse, M. B.; Natile, G. *Inorg. Chem.* **2008**, *47*, 4909–4917.

HOD peak). IR spectra were obtained with a Perkin-Elmer Spectrum One Infrared Spectrophotometer using KBr as a solid support for pellets. Elemental analyses were performed with a Carlo Erba Elemental Analyzer model 1106 instrument. X-ray diffraction experiments were performed at  $120 \pm 2$  K using a Nonius Kappa CCD area detector situated at the window of a rotating anode (EPSRC, National Crystallographic Service, School of Chemistry, University of Southampton, Southampton, U.K.), equipped with a low temperature device, Oxford Instrument Cryo-stream.<sup>26</sup>

**Starting Materials.** Commercial reagent-grade chemicals were used as received.

**Synthesis of the Me<sub>2</sub>dab Ligand.** The unmethylated (±)-dab ligand was prepared by the reduction of dimethylglyoxime with Raney nickel, followed by fractional crystallization of the HCl salt to separate the racemic from the meso form.<sup>27</sup> The racemic form was then converted to (±)-Me<sub>2</sub>dab by a three-step procedure as reported below:

- (i) Conversion of the diamine in the corresponding bis-trifluoroacetamide derivative. A solution of (±)-dab (0.55 g, 6.24 mmol) in diethyl ether (100 mL) was cooled to 0 °C and treated with trifluoroacetic anhydride (3.93 g, 18.72 mmol). The mixture was brought to 25 °C, left under stirring for 3 h, and then evaporated to dryness. The solid residue was washed repeatedly with water and dried (yield 95%). Anal. Calcd for C<sub>8</sub>H<sub>10</sub>F<sub>6</sub>N<sub>2</sub>O<sub>2</sub>: C, 34.30; H, 3.60; N, 10.00%. Found: C, 34.63; H, 3.83; N, 10.32%. <sup>1</sup>H NMR (chloroform-*d*, ppm): 6.68 (NH), 3.99 (CH), 1.30 (CCH<sub>3</sub>).
- (ii) Methylation of the amidic nitrogens. The bis-trifluoroacetamide derivative prepared in step i (0.28 g, 1 mmol) was dissolved in dimethylsulfoxide (5 mL) and then treated with powdered KOH (0.124 g, 2.2 mmol) under vigorous stirring. The clear solution obtained was treated with CH<sub>3</sub>I (0.30 g, 2.1 mmol) and the mixture left under stirring at 25 °C for 15 h. Precipitation of the trifluoroacetyl derivative was obtained by the addition of water (50 mL) to the dimethylsulfoxide solution. The solid was recovered by filtration of the mother liquor, and the crude material was extracted with *n*-hexane (100 mL). The *n*-hexane extract was evaporated to dryness under reduced pressure to leave a white powder of the desired compound. Anal. Calcd for C<sub>10</sub>H<sub>14</sub>F<sub>6</sub>N<sub>2</sub>O<sub>2</sub>: C, 38.98; H, 4.58; N, 9.09%. Found: C, 38.65; H, 4.73; N, 9.32%. <sup>1</sup>H NMR (chloroform-*d*, ppm): 4.75 (CH), 2.94 (NCH<sub>3</sub>), 1.25 (CCH<sub>3</sub>).
- (iii) Hydrolysis of the bis-amide to give the methylated diamine. The compound prepared in step ii was suspended in a mixture of concentrated hydrochloric acid and methanol (1:1 v/v, 0.2 L) and heated to reflux for about 3 h. The formed dihydrochloride derivative of the diamine, (±)-Me<sub>2</sub>dab·2HCl, was recovered by evaporation of the solution under reduced pressure. Anal. Calcd for C<sub>6</sub>H<sub>18</sub>N<sub>2</sub>Cl<sub>2</sub>: C, 38.10; H, 9.60; N, 14.81%. Found: C, 37.73; H, 9.83; N, 14.82%. <sup>1</sup>H NMR (D<sub>2</sub>O, ppm): 3.70 (CH), 2.78 (NCH<sub>3</sub>), 1.36 (CCH<sub>3</sub>).

**Synthesis of the Complexes.** [PtCl<sub>2</sub>{(±)-Me<sub>2</sub>dab}]. Dimethylsulfoxide (DMSO, 0.156 g, 2 mmol) was added to a stirred solution of K<sub>2</sub>[PtCl<sub>4</sub>] (0.415 g, 1 mmol) in water (20 mL) and the reaction mixture maintained at 70 °C, while the solution, initially reddish, turned yellow because of the formation of [PtCl<sub>2</sub>(DMSO)<sub>2</sub>]. The yellow solution was then treated with an aqueous solution of (±)-Me<sub>2</sub>dab, obtained from (±)-Me<sub>2</sub>dab·2HCl (1 mmol) neutralized with LiOH (2 mmol), added slowly over a period of 5 min. The mixture was left under stirring at 90 °C for 1 h. The yellow

precipitate that formed was collected by filtration of the mother liquor; washed with water, dimethylformamide, and diethyl ether; and dried. Yield > 80%. Anal. Calcd for C<sub>6</sub>H<sub>16</sub>N<sub>2</sub>Cl<sub>2</sub>Pt: C, 18.85; H, 4.21; N, 7.33%. Found: C, 18.52; H, 4.23; N, 7.10%. <sup>1</sup>H NMR (dimethylsulfoxide-*d*<sub>6</sub>, ppm): 5.90 (NH), 2.54 (NCH<sub>3</sub>), 2.27(CH), 1.17 (CCH<sub>3</sub>).

[Pt(NO<sub>3</sub>)<sub>2</sub>{(±)-Me<sub>2</sub>dab}]. A suspension of [PtCl<sub>2</sub>{(±)-Me<sub>2</sub>dab}] (0.170 g, 0.45 mmol) in acetone (40 mL) was treated with AgNO<sub>3</sub> (0.153 g, 0.90 mmol) dissolved in the minimum volume of water. The solution was left under stirring for 12 h. Meanwhile, the yellow color of [PtCl<sub>2</sub>{(±)-Me<sub>2</sub>dab}] disappeared, and a white precipitate of AgCl formed. The solution was filtered and evaporated to dryness, affording a white solid of [Pt(NO<sub>3</sub>)<sub>2</sub>{(±)-Me<sub>2</sub>dab}]. Anal. Calcd for C<sub>6</sub>H<sub>16</sub>N<sub>4</sub>O<sub>6</sub>Pt: C, 16.56; H, 3.70; N, 12.87%. Found: C, 16.80; H, 3.64; N, 12.88%.

[Pt{(±)-Me<sub>2</sub>dab}(9-EtG)<sub>2</sub>](NO<sub>3</sub>)<sub>2</sub>. Typically, a stock solution of 9-EtG (from commercial source) was prepared at pH ~ 1.6. An aliquot of this stock solution was then added to a reaction vessel containing the required amount of [Pt(NO<sub>3</sub>)<sub>2</sub>{(±)-Me<sub>2</sub>dab}], synthesized as described above. The progress of the reaction at ambient temperature was monitored by <sup>1</sup>H NMR spectroscopy. A typical reaction time was ~1–3 h, but the solution was kept for one day to ensure complete reaction. Then, the sample was lyophilized and analyzed. Anal. Calcd for C<sub>20</sub>H<sub>36</sub>N<sub>14</sub>O<sub>8</sub>Pt·H<sub>2</sub>O: C, 29.52; H, 4.45; N, 24.09%. Found: C, 29.13; H, 4.73; N, 24.38%.

Crystals suitable for X-ray analysis were obtained by slow evaporation of a mixture of water and methanol (1:1, v:v).

**X-Ray Crystallography.** A well-formed colorless rod of dimensions 0.15 × 0.05 × 0.05 mm was mounted on a glass fiber and then submitted to X-ray diffraction experiments at  $120 \pm 2$  K. Data were collected to a maximum 2θ value of 55° and processed through the SAINT-2<sup>28</sup> and XPREP<sup>29</sup> software packages, whereas absorption corrections were performed using SADABS.<sup>30</sup>

The structure solution and refinement were carried out via SHELX-97<sup>29</sup> by using the direct methods followed by series of difference-Fourier synthesis and least-squares cycles. The disorder of one nitrate anion (numbered 2 in the text) was solved without any restraint on the geometrical parameters. The nitrogen and one oxygen atom were given a site occupancy factor (sof) of 1, whereas the other four positions for oxygen atoms were given a sof of 0.5. All of the hydrogen atoms were located through the HFIX and AFIX options of SHELX-97 and restrained to ride on the atoms to which they are bound. Their thermal parameters were refined isotropically, and the values were 1.2 times those of the respective nitrogen or carbon atom to which they are bound. All of the non-hydrogen atoms were refined anisotropically. This model converged to final conventional agreement factors R1 = 0.0270 and wR2 = 0.0565. All computations relevant to the X-ray analyses were performed via the WinGX software package<sup>31</sup> implemented on Pentium machines operating under the Windows XP system. Selected crystallographic data are given in Table 1.

## Results

**X-Ray Structure.** The molecular structure of [Pt{(R,S,S,R)-Me<sub>2</sub>dab}(9-EtG)<sub>2</sub>]<sup>2+</sup> is depicted in Figure 2; selected bond distances and angles are listed in Table 2. The compound has the rather rare HH conformation of the

(28) Sheldrick, G. M. *SAINTPPLUS*, version 6.02; Bruker AXS: Madison, WI, 1997.

(29) Sheldrick, G. M. *SHELXS/L-97*; University of Göttingen: Göttingen, Germany, 1997.

(30) Sheldrick, G. M. *SADABS*; University of Göttingen: Göttingen, Germany, 1998.

(31) (a) Farrugia, L. J. *WinGX*, version 1.64.05; University of Glasgow: Glasgow, U. K., 1999–2003. (b) Farrugia, L. J. *J. Appl. Crystallogr.* **1999**, *32*, 837–838.

(26) Cosier, J.; Glazer, A. M. *J. Appl. Crystallogr.* **1986**, *19*, 105–110.

(27) Dickey, F. H.; Fickett, W.; Lucas, H. J. *J. Am. Chem. Soc.* **1952**, *74*, 944.

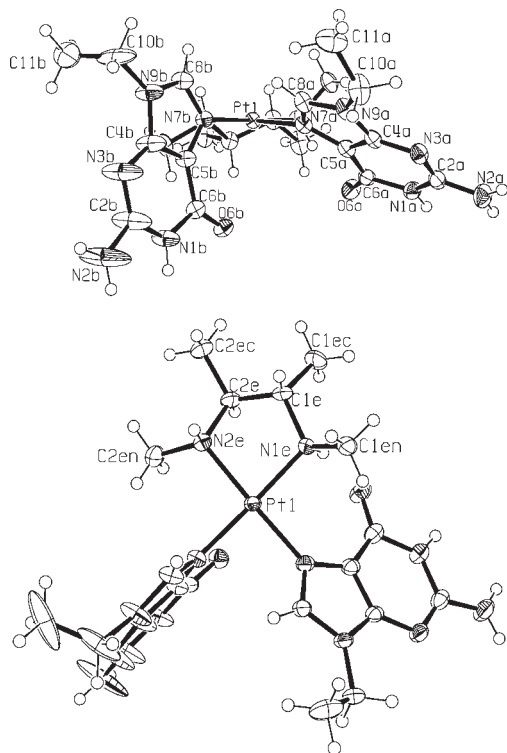


**Figure 2.** Ortep drawing of the complex molecule  $[\text{Pt}\{(R,S,S,R)\text{-Me}_2\text{dab}\}-(9\text{-EtG})_2]^{2+}$  as viewed along the line that bisects the  $\text{N7A-Pt-N7B}$  angle from the guanine side (top) and perpendicular to the coordination plane (bottom). The ellipsoids enclose 50% probability.

**Table 1.** Selected Crystallographic Data for  $[\text{Pt}\{(\pm)\text{-Me}_2\text{dab}\}(9\text{-EtG})_2](\text{NO}_3)_2$

| parameter   | value  |
|---|--|
| empirical formula   | $\text{C}_{20}\text{H}_{34}\text{N}_{14}\text{O}_8\text{Pt}$ |
| fw  | 793.70   |
| temp/K  | 120(2)   |
| wavelength/Å  | 0.71073  |
| cryst syst  | monoclinic   |
| space group   | $P2_1/n$   |
| unit cell dimensions  |  |
| $a/\text{Å}$  | 8.8521(4)  |
| $b$   | 16.869(2)  |
| $c$   | 19.526(2)  |
| $\beta/\text{deg}$  | 98.522(6)  |
| vol/Å <sup>3</sup>  | 2883.5(4)  |
| $Z$   | 4  |
| calcd density/Mg m <sup>-3</sup>                            | 1.828  |
| absn coeff/mm <sup>-1</sup>                                 | 4.936  |
| $F(000)$  | 1576   |
| cryst size/mm <sup>3</sup>                                  | 0.15 × 0.05 × 0.05   |
| reflns collected/unique                                     | 42872/6592 [R(int) = 0.0473]                                 |
| refinement method   | full-matrix least-squares on $F^2$                           |
| data/restraints/parameters                                  | 6592/0/407   |
| goodness-of-fit on $F^2$                                    | 1.022  |
| final R indices [ $I > 2\sigma(I)$ ]                        | R1 = 0.0270, wR2 = 0.0565                                    |
| R indices (all data)  | R1 = 0.0322, wR2 = 0.0588                                    |
| largest diff. peak and hole e <sup>-</sup> ·Å <sup>-3</sup> | 1.362 and -1.048   |

guanine bases, which, combined with the  $C_2$  symmetry of the diamine ligand, has allowed us to see in detail the different stereochemistry stemming from having either the C8-H or the six-membered ring of the guanine on the same side of the coordination plane as the Me substituent on the *cis* amine.

**Platinum Coordination.** The platinum center has the usual square-planar coordination. The sum of the four consecutive bond angles in the plane is  $360.1(1)^\circ$ , and the

**Table 2.** Selected Bond Lengths (Å) and Angles (deg) for  $[\text{Pt}\{(\pm)\text{-Me}_2\text{dab}\}-(9\text{-EtG})_2](\text{NO}_3)_2$

| vector      | length   |
|-------------|----------|
| Pt1-N7A     | 2.044(3) |
| Pt1-N7B     | 2.016(3) |
| Pt1-N1E     | 2.030(3) |
| Pt1-N2E     | 2.038(3) |
| O6A-C6A     | 1.228(4) |
| O6B-C6B     | 1.215(4) |
| N1A-C2A     | 1.376(5) |
| N1B-C2B     | 1.365(5) |
| N2A-C2A     | 1.337(5) |
| N2B-C2B     | 1.339(5) |
| N7A-C8A     | 1.318(4) |
| N7B-C8B     | 1.315(4) |
| N9A-C10A    | 1.477(4) |
| N9B-C10B    | 1.468(5) |
| vectors     | angle    |
| N7A-Pt1-N7B | 88.4(1)  |
| N1E-Pt1-N7A | 93.9(1)  |
| N1E-Pt1-N2E | 84.0(1)  |
| N7B-Pt1-N2E | 93.8(1)  |
| C5A-N7A-Pt1 | 130.1(2) |
| C5B-N7B-Pt1 | 126.7(2) |
| C8A-N7A-Pt1 | 124.2(3) |
| C8B-N7B-Pt1 | 127.0(2) |
| N7A-C5A-C6A | 133.3(3) |
| N7B-C5B-C6B | 131.0(3) |
| O6A-C6A-C5A | 130.3(3) |
| O6B-C6B-C5B | 128.9(3) |

metal center is displaced from the plane of the four donor atoms by only 0.019(1) Å. The platinum-amine bond distances (average value 2.034(3) Å) are equal within 2 times the standard deviation and are in agreement with previous values found for the  $[\text{Pt}(\text{dimethylmalonato})\{(\pm)\text{-}2,2'\text{-bipiperidine}\}]$  complex.<sup>25</sup> A significant difference is observed between the Pt-N7 bond lengths (0.028(3) Å), the more canted guanine (A) having the longer bond. The metal center deviates only slightly from the guanine planes. The deviation is larger for guanine-A (0.143(1) Å) than for the less canted guanine-B (0.036(1) Å).

**Me<sub>2</sub>dab Ligand.** Bond lengths and angles are normal for this type of ligand. The puckering of the chelate ring,  $q_2 = 0.442(3)$  Å,<sup>32</sup> is normal when compared to other Pt-ethylenediamine ligands. It is to be noted that the configuration at the N atom is induced by that of the adjacent C atom during coordination of the diamine to platinum and formation of the chelate ring. Both the *R,S,S,R* and *S,R,R,S* configurations at the N,C,C,N chelate-ring atoms are present in the crystal; however, only the former is shown in Figure 2. In turn, the  $\delta$  or  $\lambda$  puckering of the chelate ring is determined by the *R,S,S,R* or *S,R,R,S* configuration of the chelate ring atoms. A detailed analysis of the steric factors will be given in the Discussion section.

**9-EtG Ligands.** The endocyclic atoms of the two guanine systems define two good least-squares planes, the deviations from planarity being  $\leq 0.030(4)$  Å. Also, the exocyclic atoms do not deviate significantly from the least-squares planes, the largest deviation being that of N2A (0.096(3) Å). The orientation of the two guanines is head-to-head, but their canting is very different, forming a dihedral angle with the coordination plane of  $35.7(1)^\circ$  (N1E-Pt1-N7A-C5A torsion angle of  $35.2(2)^\circ$ ) for guanine-A and of  $83.6(1)^\circ$  (N2E-Pt1-N7B-C5B torsion angle of  $95.6(3)^\circ$ )

(32) Cremer, D.; Pople, J. A. *J. Am. Chem. Soc.* **1975**, *97*, 1354-1358.

for guanine-B. The dihedral angle between guanine planes is  $85.2(1)^\circ$ .

It should be noted that, owing to the different canting of the guanine bases with respect to the coordination plane, the O6B atom is much closer to the Pt atom ( $\text{Pt}1 \cdots \text{O6B}$ ,  $3.372(3) \text{ \AA}$ ) than the O6A atom ( $\text{Pt}1 \cdots \text{O6A}$ ,  $3.620(3) \text{ \AA}$ ). The distance of  $3.372 \text{ \AA}$  is very close to the sum of the van der Waals radii for oxygen ( $1.5 \text{ \AA}$ ) and platinum ( $1.7\text{--}1.8 \text{ \AA}$ ),<sup>33</sup> thus the existence of an attractive interaction between Pt1 and O6B cannot be excluded and appears to be supported by the values of the angles  $\text{N7B-C5B-C6B}$  ( $131.0(3)^\circ$ ) and  $\text{C5B-C6B-O6B}$  ( $128.9(3)^\circ$ ), which are narrower than corresponding  $\text{N7A-C5A-C6A}$  ( $133.3(3)^\circ$ ) and  $\text{C5A-C6A-O6A}$  ( $130.3(3)^\circ$ ) angles in guanine-A. In previously reported platinum complexes with guanine derivatives,  $\text{Pt} \cdots \text{O}$  contact distances as short as  $3.526(7) \text{ \AA}$ <sup>34</sup> and  $3.39(1) \text{ \AA}$ <sup>35</sup> (the latter only slightly longer than that observed in the present case) were found. A  $\text{Pt} \cdots \text{O}$  distance of  $3.474(6) \text{ \AA}$  was found for one of the two guanine bases in the complex  $[\text{Pt}(\text{ethylenediamine})\{9\text{-(HO-CH}_2\text{-CH}_2\text{-O-CH}_2\text{)G}\}_2]$ , also having the HH conformation, and for which the existence of an attractive  $\text{Pt} \cdots \text{O6}$  interaction was also supported by DFT molecular orbital calculations.<sup>36</sup> Finally, an electrostatic interaction has been demonstrated to take place between a rather similar platinum substrate ( $[\text{Pt}(\text{NH}_3)_4]^{2+}$ ) and an axial  $\text{H}_2\text{O}$  molecule.<sup>37</sup> Guanine-B has very little canting (it is nearly orthogonal to the coordination plane) with the six-membered ring slightly rotated (by ca.  $5^\circ$ ) toward the *cis* guanine. Such a positioning of the guanine reduces steric interactions between the six-membered ring of the guanine and the methyl substituent on the *cis* amine (shorter nonbonding interaction of  $2.90(1) \text{ \AA}$  between methyl protons of the amine and C5 atom of the guanine), while allowing for an attractive interaction between the O6 of guanine-B and the platinum center. Thanks to the high canting of the second guanine, nonbonding interactions between six-membered rings of the two guanines remain low (distance of  $4.34(1) \text{ \AA}$  between O6 atoms of the two guanines).

As anticipated, guanine-A is highly canted ( $\text{N1-Pt-N7A-C5A}$  torsion angle of  $35.2^\circ$ ). A driving force to such a high canting is the relief of steric interaction between  $\text{C8-H}$  and *cis*  $\text{N-Me}$  (both on the same side of the platinum coordination plane) and, even more, the formation of a strong hydrogen bond between guanine and *cis* amine ( $\text{N1E} \cdots \text{O6A}$ ,  $2.752(4) \text{ \AA}$ ;  $(\text{N1E})\text{H} \cdots \text{O6A}$ ,  $1.90(1) \text{ \AA}$ ;  $\text{N-H} \cdots \text{O}$ ,  $154.7(4)^\circ$ ). Because the canting of guanine-A moves the six-membered ring outward from the *cis* guanine, we call this type of canting "six out". The high canting of guanine-A brings the  $\text{C8A-H}$  atom quite close to  $\text{C8B}$  ( $\text{H} \cdots \text{C}$  distance of  $2.80(1) \text{ \AA}$ , at the limit of the sum of the van der Waals radii totaling  $2.85 \text{ \AA}$ <sup>33</sup>).

In a previous investigation concerning bis-guanine derivatives of oxaliplatin,<sup>38</sup> it was shown that the guanine  $\text{O6-NH}$  *cis* amine H-bond interaction is stronger when the  $\text{N-H}$  is "quasi axial" and the guanine is deprotonated at N1 (increased H-bond acceptor capacity of O6). Also, in our case, the  $\text{N-H}$  forming the H bond with guanine-A is "quasi axial"; therefore the conditions for H-bond formation are the best as far as the stereochemistry of  $\text{N-H}$  is concerned. Although the  $\text{N-H}$  is "quasi axial", guanine-A is forced to be strongly canted (dihedral angle with the coordination plane of  $35.7(1)^\circ$ ) in order to reach the situation in which the  $\text{N-H}$  proton falls in the plane of the guanine, which is also the plane of the O6 lone pairs of electrons. Such a high canting could have the effect of increasing the repulsion between the guanine ligand and the platinum moiety, and this could explain the lengthening of the  $\text{Pt-N7}$  bond, which is  $0.028(3) \text{ \AA}$  longer for guanine-A than for guanine-B, which instead has an ideal nearly orthogonal orientation of the base plane with respect to the coordination plane.

**The Ethyl Groups.** The ethyl groups adopt a different conformation for the two ligands: in the case of guanine-A, it is almost eclipsed (or *-syn-periplanar*) to the  $\text{N9A-C8A}$  bond ( $\text{C8A-N9A-C10A-C11A}$  torsion angle of  $-25.6(5)^\circ$ ), whereas in the case of guanine-B, it has a *+anticlinal* orientation ( $\text{C8B-N9B-C10B-C11B}$  torsion angle of  $98.4(6)^\circ$ ). As a consequence of the steric interaction between the  $\text{C11A}$  methyl group and  $\text{C8A-H}$ , the bond angles  $\text{C11A-C10A-N9A}$  and  $\text{C10A-N9A-C8A}$  are significantly larger than the corresponding angles in guanine B.

**Intermolecular Interactions.** H bonds and  $\pi$  interactions are shown in Figure S1 of the Supporting Information. N1 and N2 of guanine-B form two good H bonds with nitrate-1 [ $\text{N1B} \cdots \text{O1N1}$ ,  $2.884(6) \text{ \AA}$ ;  $(\text{N1B})\text{H} \cdots \text{O1N1}$ ,  $2.02(2) \text{ \AA}$ ;  $\text{N1B-H} \cdots \text{O1N1}$ ,  $178.1(5)^\circ$ ;  $\text{N2B} \cdots \text{O3N1}$ ,  $2.979(6) \text{ \AA}$ ;  $(\text{N2B})\text{H} \cdots \text{O3N1}$ ,  $2.16(3) \text{ \AA}$ ;  $\text{N2B-H} \cdots \text{O3N1}$ ,  $159.6(5)^\circ$ ]. The same guanine is involved in a  $\pi$  interaction with a symmetry-related nitrate-2 (II in Figure S1): [shortest  $\text{C2B} \cdots \text{O5N2}(-x + 2.5, y - 0.5, -z + 0.5)$  distance of  $2.72(3) \text{ \AA}$ , while the van der Waals radii are  $1.50$  and  $1.65 \text{ \AA}$  for O and C, respectively<sup>33</sup>]. N2 of guanine-A forms H bonds with nitrate-2 (this nitrate is statistically disordered with fixed positions only for N2 and O1 and two sites with a *sof* of 0.5 for each one of the other two oxygens) [ $\text{N2A} \cdots \text{O1N2}$ ,  $3.048(5) \text{ \AA}$ ;  $(\text{N2A})\text{H} \cdots \text{O1N2}$ ,  $2.24(2) \text{ \AA}$ ;  $\text{N2A-H} \cdots \text{O1N2}$ ,  $157.5(2)^\circ$ ;  $\text{N2A} \cdots \text{O2N2}$ ,  $2.994(7) \text{ \AA}$ ;  $(\text{N2A})\text{H} \cdots \text{O2N2}$ ,  $2.41(2) \text{ \AA}$ ;  $\text{N2A-H} \cdots \text{O2N2}$ ,  $125.4(3)^\circ$ ]. N1 and N2 of the same guanine-A form good H bonds with a symmetry-related nitrate-1 (I in Figure S1) [ $\text{N1A} \cdots \text{O2N1}(-x + 2, -y + 2, -z)$ ,  $2.809(5) \text{ \AA}$ ;  $(\text{N1A})\text{H} \cdots \text{O2N1}$ ,  $2.09(2) \text{ \AA}$ ;  $\text{N1A-H} \cdots \text{O2N1}$ ,  $140.8(4)^\circ$ ;  $\text{N2A} \cdots \text{O1N1}(-x + 2, -y + 2, -z)$ ,  $3.006(6) \text{ \AA}$ ;  $(\text{N2A})\text{H} \cdots \text{O1N1}$ ,  $2.15(2) \text{ \AA}$ ;  $\text{N2A-H} \cdots \text{O1N1}$ ,  $169.7(5)^\circ$ ].

**Spectroscopy.** The  $^1\text{H}$  NMR spectrum of  $[\text{Pt}\{\pm\}\text{Me}_2\text{dab}\{\text{NO}_3\}_2]$  in  $\text{D}_2\text{O}$  at pH 3.3 has one set of signals from the two magnetically equivalent halves of  $\text{Me}_2\text{dab}$  (a broad NH singlet at 6.15 ppm, a CH multiplet at 2.51 ppm, and  $\text{NCH}_3$  and  $\text{CCH}_3$  doublets at 2.49 and 1.20 ppm). The spectrum is consistent with the presence of  $[\text{Pt}\{\pm\}\text{Me}_2\text{dab}\{\text{D}_2\text{O}\}_2]^{2+}$  in solution. The  $[\text{Pt}\{\pm\}\text{Me}_2\text{dab}\{9\text{-EtG}\}_2(\text{NO}_3)_2$  sample has a spectrum with multiple H8 signals characteristic of different atropisomers. In the pH

(33) Bondi, A. J. *Phys. Chem.* **1964**, *68*, 441–451.

(34) Shollhorn, H.; Raudaschl-Sieber, G.; Müller, G.; Thewalt, U.; Lippert, B. *J. Am. Chem. Soc.* **1985**, *107*, 5932–5937.

(35) Sherman, S. E.; Gibson, D.; Wang, A. H. -J.; Lippard, S. J. *Science* **1985**, *230*, 412–418.

(36) Cini, R.; Grabner, S.; Bukovec, N.; Cerasino, L.; Natile, G. *Eur. J. Inorg. Chem.* **2000**, 1601–1607.

(37) Kozelka, J.; Bergès, J.; Attias, R.; Fraita, J. *Angew. Chem., Int. Ed. Engl.* **2000**, *39*, 198–201.

(38) Benedetti, M.; Marzilli, L. G.; Natile, G. *Chem.—Eur. J.* **2005**, *11*, 5302–5310.

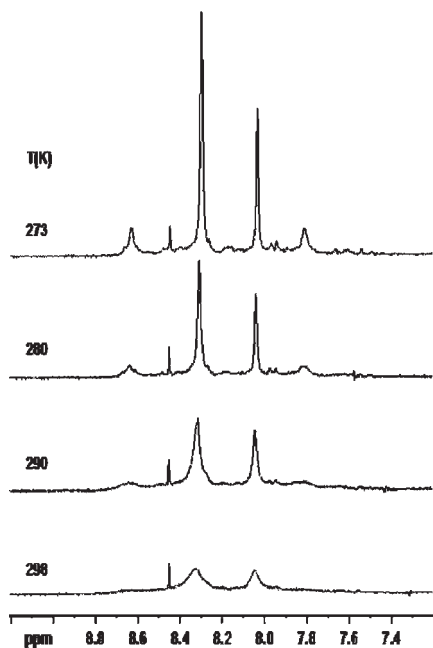


**Figure 3.**  $^1\text{H}$  NMR spectrum ( $\text{D}_2\text{O}$  solution) in the region of C8–H signals for  $[\text{Pt}\{(\pm)\text{-Me}_2\text{dab}\}(9\text{-EtG})_2](\text{NO}_3)_2$  at temperatures between 273 K (top) and 298 K (bottom). The low intensity signal at 8.45 ppm belongs to free 9-EtG.

$\sim 1\text{--}3.5$  range, the H8 signals do not exhibit a pH-dependent shift, an indication that the N7 of 9-EtG is coordinated to Pt and cannot become protonated. Atropisomers expected for bis adducts of the type  $[\text{Pt}\{(\pm)\text{-Me}_2\text{dab}\}(9\text{-EtG})_2]^{2+}$  are shown in Figure 1. Each  $C_2$ -symmetrical HT atropisomer has one set of  $^1\text{H}$  NMR signals. For the HH atropisomer, two different H8 signals and two signals from the  $\text{NCH}_3$ ,  $\text{NH}$ ,  $\text{CCH}_3$ , and  $\text{CH}$  groups of  $(\pm)\text{-Me}_2\text{dab}$  are possible.

Only two large broad H8 signals are present at 25 °C in the  $^1\text{H}$  NMR spectrum of a solution containing  $[\text{Pt}\{(\pm)\text{-Me}_2\text{dab}\}(9\text{-EtG})_2]^{2+}$ . At 0 °C, these H8 signals sharpened, and two additional H8 signals of equal intensity emerged (Figure 3). Integration gave 2.9:1.5:1 for HT major (8.22 ppm)/HT minor (7.96 ppm)/HH (7.74 and 8.55 ppm). Other signals include  $\text{NH}$  for HT major (6.01 ppm, the acidic pH lowers the rate of exchange of the  $\text{NH}$  proton with  $\text{D}_2\text{O}$ ), HT minor (5.71 ppm), and HH (5.82/6.12 ppm);  $\text{NCH}_3$  for HT major (2.30 ppm) and HT minor (2.35 ppm);  $\text{CH}$  for HT major (2.78 ppm) and HT minor (2.86 ppm); and  $\text{CCH}_3$  for HT major (1.29 ppm) and HT minor (1.29 ppm). The Et signals were not resolved for each atropisomer and appeared at 4.06 ( $\text{CH}_2$ ) and 1.35 ( $\text{CH}_3$ ) ppm.

## Discussion

### Induction of Asymmetry within the Chelate Diamine.

Although the  $\text{Me}_2\text{dab}$  ligand has made a great contribution to the characterization of possible conformers in dynamic *cis*- $\text{A}_2\text{PtG}_2$  derivatives ( $\text{A}_2$  = two amines or a diamine and  $\text{G}_2$  = two detached or tethered guanine bases), a detailed description of the synthesis of this ligand has never been given. Now, this is reported in the Experimental Section.

Any given amine could in theory adopt either the *R* or *S* configuration, and the chelate ring pucker could have either the  $\delta$  or  $\lambda$  chirality. However, as anticipated in the Results section, within the chelate ring, the configuration

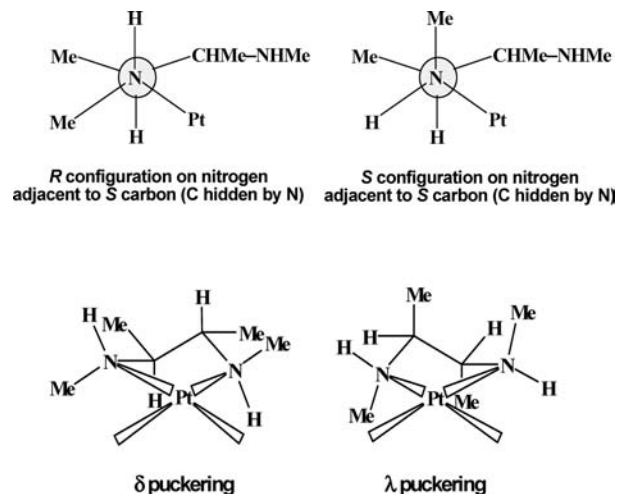


**Figure 4.** Top: Schematic drawing of lower crowding of substituents on adjacent C and N atoms when the two atoms have opposite configurations (*S* and *R*, left) versus when the two atoms have the same configuration (*S*, right). Bottom: Schematic drawing of  $\delta$  and  $\lambda$  puckering of the chelate ring for (*R,S,S,R*)- $\text{Me}_2\text{dabPt}$  complexes. The switch from  $\delta$  (left) to  $\lambda$  (right) puckering causes translocation of methyl substituents from “quasi equatorial” to “quasi axial” positions; this latter conformation is destabilized by strong steric repulsions between Me substituents in positions 1,3 of the chelate ring.

of the N atoms is induced by that of the adjacent C atom, and the  $\delta$  or  $\lambda$  puckering of the chelate ring is determined by the resulting *R,S,S,R* or *S,R,R,S* configuration at the chelate ring N,C,C,N atoms. As shown in Figure 4, for a given configuration at carbon (e.g., *S*) and for the requirement that a cisoid disposition of the platinum and distal nitrogen exists in order to allow for chelation, the *R* configuration on the coordinated nitrogen (top-left sketch) ensures a less sterically crowded situation than that obtained if the latter nitrogen adopts the *S* configuration (top-right sketch). This leads to the *R* configuration for N adjacent to the C atom with *S* configuration and, *vice versa*, to *S* configuration for N adjacent to the C atom with the *R* configuration.

Always for steric reasons (reduction of nonbonding interaction between axial substituents in positions 1 and 3 of the chelate ring), the methyl substituents on the chelate ring will tend to occupy “quasi equatorial” positions (and, conversely, hydrogen substituents “quasi axial” positions). As a consequence, for *R,S,S,R* configuration of the carbon and nitrogen atoms of the chelate ring, the chelate ring puckering will be  $\delta$  (which places methyl substituents in 1,3 positions of the chelate ring in bis-equatorial positions, bottom-left sketch of Figure 4) rather than  $\lambda$  (which places methyl substituents in 1,3 positions of the chelate ring in bis-axial positions, bottom-right sketch of Figure 4). In contrast, for the *S,R,R,S* configuration of the chelate ring atoms, the preferred puckering will be  $\lambda$ . The configuration and puckering of the diamine remain stable in all reactions at the metal center, which does not involve opening of the chelate ring.

**The  $\text{Me}_2\text{dab}$  Ligand Influences the Canting of the Guanines.** The chirality of the chelate ligand determines the *L* or *R* canting of the nucleobases (with reference to two straight lines, one passing through N1 and C8 of a guanine and the other through the N7 atoms of the two coordinated guanines, *L* or *R* canting indicates that the two lines are described by the thumb and index of the left or right hand,

respectively; bottom sketch of Figure 1). In the following discussion, we will refer to the isomer with the *R,S,S,R* configuration of Me<sub>2</sub>dab (the one shown in Figure 2 and in the bottom sketch of Figure 1). The results apply also to the *S,R,R,S* isomer but with inverted chiralities. Thus, *R,S,S,R*-Me<sub>2</sub>dab will induce *R* canting because this reduces steric interaction between the amine N–Me and the portion of the *cis* guanine [either the six-membered ring (guanine-B) or C8–H (guanine-A)] that is on the same side of the platinum coordination plane. It turns out that for guanine-B the six-membered ring is directed toward the *cis* guanine, and we call this conformation “six-in”. For guanine-A, the six-membered ring moves away from the *cis* guanine, and we call this conformation “six-out”. Moreover, guanine-A can form a strong guanine O6–NH *cis* amine H bond. Therefore, both guanines of the HH atropisomer have *R* canting (determined by the *R,S,S,R* configuration of the diamine), and as a consequence, one guanine is canted “six-in” and the other “six-out”. The “six-in” guanine will have C8–H moving away from the *cis* guanine (and its shielding zone) and will give a downfield-shifted <sup>1</sup>H NMR signal. In contrast, the “six-out” guanine will have C8–H moving toward the *cis* guanine (and deeper inside its shielding zone) and will give an upfield-shifted signal (see later section on H8 chemical shifts).

**From the HH to the HT Conformers.** Starting from the X-ray structure of the HH conformer with *R,S,S,R* configuration of the Me<sub>2</sub>dab ligand (Figure 2), in a gedanken experiment, we can rotate guanine-A counterclockwise until it reaches the conformation C<sub>2</sub>-symmetrical with respect to guanine-B. The resulting HT conformer will have Δ chirality (orientations of the axis connecting the O6 atoms of the two guanines and the perpendicular to the coordination plane passing through the platinum atom described by the thumb and index of the right hand). The canting of the two guanine bases will remain *R*, but both guanines will now have the “six-in” conformation. The degree of canting will be initially small (since it was small for guanine B in the HH atropisomer); however, there is no apparent impediment to a greater “six-in” canting of the two guanines because for both guanines C8–H is on the same side of NH of the *cis* amine with respect to the platinum coordination plane, and there is no building up of repulsive interaction between the two moieties. Moreover, a greater “six-in” canting of the two guanines could have the beneficial effect of increasing the attractive interaction between the H8 of a guanine (with low electron density) and the O6 of the *cis* guanine (with high electron density) by reducing the distance between the two moieties (increased dipole–dipole interaction). Furthermore, by increasing the “six-in” canting of the two guanines, the dihedral angle between the planes of the two guanines decreases while the overlapping increases. This increased canting would have the effect of increasing the stacking interaction between the two bases. Such a “six-in” canting can reach rather large values, as indicated by the low dihedral angle (53° and 48°) between the guanine plane and the coordination plane in [Pt(dap)(Me-5'-GMP)<sub>2</sub>] (dap = 1,3-diaminopropane, Me-5'-GMP = 5'-guanosine monophosphate methyl

ester)<sup>39</sup> and [Pt(en)(5'-GMP)<sub>2</sub>] (en = ethylenediamine),<sup>40</sup> respectively. In both of these latter cases, the C8–H of each guanine was on the same side of the platinum-coordination plane as an N–H of the *cis* amine.

Always starting from the HH conformer and *R,S,S,R* configuration of the Me<sub>2</sub>dab ligand (Figure 2), in a gedanken experiment, we can rotate clockwise guanine-B until it reaches the conformation C<sub>2</sub>-symmetrical with respect to guanine-A. The resulting HT conformer will have Λ chirality (orientations of the axis connecting the O6 atoms of the two guanines and the perpendicular to the coordination plane passing through the platinum atom described by the thumb and index of the left hand). The canting of the two guanines will remain *R*, but both guanines will have the six-membered ring directed outward from the *cis* guanine (“six-out” conformation). The degree of canting will be very large (it was very large already for guanine A in the HH isomer), and both guanines will be able to form a strong H bond with the *cis* amine through O6. In this highly canted conformation, the dihedral angle between the planes of the two guanines is rather small, but the overlapping between the two bases is small because of the “six-out” conformation. Therefore, the π-stacking interaction is also small. Furthermore, the dipole–dipole interaction between the two guanines cannot contribute to the stability of this highly canted conformer because the electron-deficient C8–H of one guanine is closer to the C8–H, rather than to the O6, of the *cis* guanine. In conclusion, this ΔHT conformer can benefit only from the H-bond interaction between the O6 of each guanine and the *cis* amine. In order to benefit from dipole–dipole and stacking interactions between *cis* guanines, this ΔHT conformer must switch to a significantly canted “six-in” conformation, but this switch encounters an obstacle in creating a steric repulsion between guanine C8–H and *cis* amine N–Me, both groups being on the same side of the platinum coordination plane, therefore the conformation of this atropisomer will likely remain “six-out”. Such was not the case for the ΔHT atropisomer previously discussed, for which the guanine C8–H was on the same side of the coordination plane as the NH of the *cis* amine.

**Guanine Canting, Stability of Atropisomers, and H8 Chemical Shifts.** NMR and CD data (the latter in the case of derivatives with enantiomerically pure Me<sub>2</sub>dab and bip ligands) reported in previous works and confirmed in the present investigation<sup>16</sup> have shown that the HT conformer with the “six-in” conformation of the guanine bases (C8–H on the same side of the coordination plane as the N–H of the *cis* amine) is favored over the HT conformer with the “six-out” conformation (C8–H on the same side of the coordination plane as the N-alkyl substituent of the *cis* amine), indicating that dipole–dipole and stacking interactions between *cis* guanines can win out over H-bond interactions between guanine and the *cis* amine. One reason the O6–NH H bonding seems to be secondary is that water is necessarily displaced from NH H bonding to allow O6–NH H-bond formation.<sup>41,42</sup>

(40) Barnham, K. J.; Bauer, C. J.; Djuran, M. I.; Mazid, M. A.; Rau, T.; Sadler, P. J. *Inorg. Chem.* **1995**, *34*, 2826–2832.

(41) Carlone, M.; Marzilli, L. G.; Natile, G. *Eur. J. Inorg. Chem.* **2005**, 1264–1273.

(42) Carlone, M.; Marzilli, L. G.; Natile, G. *Inorg. Chem.* **2004**, *43*, 584–592.

(39) Marzilli, L. G.; Chalilpoyil, P.; Chiang, C. C.; Kistenmacher, T. J. *J. Am. Chem. Soc.* **1980**, *102*, 2480–2482.

This explains the rather unexpected results of “retro model” investigations showing that (i) the more stable HT atropisomer is the one in which the bulkier six-membered ring of the guanine is on the same side of the coordination plane as the *N*-alkyl substituent of the *cis* amine and (ii) the steric interaction between C8–H (rather than the six-membered ring of the guanine) and a substituent on the *cis* amine (N–Me in the present case) dictates the stability of different HT atropisomers.

The chemical shift separation between the H8 signals of the two HT atropisomers is a consequence of their different “six-in” and “six-out” cantings. The conformer with “six-in” canting of the two guanines has C8–H moving outward from the *cis* guanine and would have a deshielded (downfield) H8 signal. In contrast, the conformer with “six-out” canting of the guanines moves C8–H in toward the *cis* guanine and would have a shielded (upfield) H8 signal. The greater the degree of canting, the greater is the chemical-shift separation. In fact, in the case of derivatives with tetra-*N*-substituted diamines, where only little canting is allowed, the chemical shift separation between the two HT atropisomers is very small ( $\leq 0.05$  ppm).<sup>43–45</sup>

The structure of the HH atropisomer also explains the large separation in chemical shift (0.81 ppm) between the H8 signals of the two guanines. The HH conformation and the same handedness of canting for the two guanines imply that, while one guanine is canted “six-in”, the other guanine is canted “six-out”. As a consequence, H8 of the former guanine moves outward from the *cis* guanine (thereby escaping its shielding zone) and is strongly deshielded; in contrast, H8 of the latter guanine moves in toward the *cis* guanine (thereby entering its shielding zone) and is strongly shielded.

## Conclusions

The X-ray structure of  $[\text{Pt}\{\pm\text{-Me}_2\text{dab}\}(9\text{-EtG})_2](\text{NO}_3)_2$  has been determined at a good level of accuracy. The structure cements the conclusion that steric relationships within the Me<sub>2</sub>dab ligand involving the fixed configuration at the chelate ring carbons account for the induction of asymmetry from the C to the N atoms and puckering of the chelate ring.

The complex molecule has the rare HH orientation of the two guanines (while the diamine has C<sub>2</sub> symmetry), allowing investigation of different intramolecular relationships between the guanine moiety and the *cis* amine. A crucial role is played by the steric interaction between the amine substituent

and the portion of the *cis* guanine that is on the same side of the platinum coordination plane. The two guanines have different degrees of canting but equal handedness of canting that is entirely determined by the chirality of the diamine ligand (*R* canting for the *R,S,S,R* configuration of the diamine and *L* canting for the *S,R,R,S* configuration). Both species are present in the crystal. For a HH conformer, the same handedness of canting implies that while one guanine is canted “six-in” and has a deshielded H8, the other guanine is canted “six-out” and has a shielded H8.

The same handedness of guanine canting of the HH conformer is shared by the two HT atropisomers, now with the consequence that while one HT conformer has “six-in” canted guanines both with a deshielded H8, the other HT conformer has “six-out” canted guanines both with a shielded H8. The “six-in” conformation favors dipole–dipole and stacking interactions between *cis* guanines. In contrast, the “six-out” conformation brings the O6 of each guanine close to the N–H of the *cis* amine with which the O6 can form a H bond. It turns out that the latter H-bond interaction is not sufficiently strong to counterbalance the loss in stability resulting from the weaker dipole–dipole and  $\pi$  interactions between *cis* guanines. The latter interactions (dipole–dipole and  $\pi$  stacking) are favored in a highly canted “six-in” conformation, which can be attained only when there is no steric repulsion between the guanine C8–H and the substituents on the *cis* amine. Therefore, it is reasonable to conclude that the latter interaction dictates which of the HT atropisomers has the greater stability in these systems.

The solid state data presented here in conjunction with the solution NMR results have greatly helped to put on a firmer base the conclusions drawn from previous “retro model” investigations, which relied most heavily on spectroscopic data obtained for solutions. Moreover, we note that a crystallographically determined structure of a HH conformer of a *cis*-[PtA<sub>2</sub>(5'-GMP)<sub>2</sub>], or indeed of any other *cis*-[metal(6-oxopurine nucleotide)<sub>2</sub>] adduct, has not yet been reported. The evidence for the existence of such an HH conformer of *cis*-[PtA<sub>2</sub>(5'-GMP)<sub>2</sub>] adducts continues to depend primarily on NMR results, which have been placed onto a firmer foundation by the results described here.

**Acknowledgment.** The authors thank the Universities of Bari and Siena, the Consorzio Interuniversitario di Ricerca in Chimica dei Metalli nei Sistemi Biologici (CIRCMSB), the Italian Ministero dell'Università e della Ricerca (FIRB RBNE03PX83 and PRIN 2006 033492), and EC (COST Action D39) for support.

**Supporting Information Available:** Drawing of the complex salt  $[\text{Pt}\{(R,S,S,R)\text{-Me}_2\text{dab}\}(9\text{-EtG})_2](\text{NO}_3)_2$  showing H-bond interactions between guanines and nitrate anions (Figure S1). This material is available free of charge via Internet at <http://pubs.acs.org>.

(43) Benedetti, M.; Saad, J. S.; Marzilli, L. G.; Natile, G. *Dalton Trans.* **2003**, 872–879.

(44) Margiotta, N.; Papadia, P.; Fanizzi, F. P.; Natile, G. *Eur. J. Inorg. Chem.* **2003**, 1136–1144.

(45) Benedetti, M.; Tamasi, G.; Cini, R.; Marzilli, L. G.; Natile, G. *Chem.—Eur. J.* **2007**, 3131–3142.